DYNAMIC CHARGING OF UNMANNED AERIAL VEHICLES USING IRS

MTP PHASE-II Report

Master of Technology

Submitted by

Omkar Amol Jadhav

Roll no.- 204102021

Advisors

Dr. Salil Kashyap

Prof. Sisir Kumar Nayak

Department of Electrical and Electronics Engineering

Indian Institute of Technology, Guwahati

ASSAM - 781039 India

June, 2022

Acknowledgement

First of all thanks to the merciful almighty for the countless gifts that you have offered me and thanks to my family for their care and support.

I'd like to use this opportunity to offer my heartfelt gratitude and appreciation to my primary supervisor Dr. Salil Kashyap for allowing me to take this idea as a project work under his valuable guidance. Without his guidance, support and knowledge, finding solution for the project problem statement would have been a difficult journey but disciplined approach can bring good results is the best learning under his teachings.The freedom to express views and communicate them provided a very conducive environment to discuss the problems and trying to find out solutions to it was the best part of this MTech journey. It was great working under him. The rational advice and support of my second supervisor Prof. Sisir Kumar Nayak has been very useful both on academic and personal level, for that I am very obliged. I am very thankful to my Father Mr. Amol Jadhav, Mother Mrs. Vaishali Jadhav and Brother Abhishek Jadhav for always supporting me in all ups and downs and has always been backbone for whatever progress I had in my career.

I'm also thankful to all of the EEE Department's faculty members for the knowledge they shared with me during the classes that helped me finish my degree. I'd like to express my gratitude to the Indian Institute of Technology, Guwahati, and its employees for their financial, academic, and technical assistance, particularly in the award of a Postgraduate Fellowship, which covered all of my expenses. It has been a fantastic and memorable journey of two years in this college. Thank you all!!

Abstract

Usage of UAV (Unmanned Aerial Vehicles) is increasing at a very rapid rate in all fields of technology. Its flexibility and cost effectiveness makes it a best possible option for usage in different fields. The increasing efficiency especially in search and rescue operations, aerial surveying, delivery system along with imaging brings it into a huge demand. But with advantages, it comes with disadvantages. It is generally a battery operated device which makes it an energy constrained device for large distances of mobility.

So as to overcome this problem we are trying to optimize and develop a system which will help to dynamically charge the UAV's using remote charging stations and IRS (Intelligent Reflecting Surfaces).We will study its feasibility in practical day to day life so that this UAV system no more remains energy constrained or mobility constrained device.

Contents

List of Figures

1 INTRODUCTION

This chapter will give brief introduction about the devices used for our system model, its working and the related literature to study them. We will discuss the fields of research to explore and formulate a problem statement to study upon.

1.1 Unmanned Aerial Vehicles (UAV)

UAV's are also known as ROA(Remotely Operated Aircraft).Presently, they are the most versatile device that can be used in almost all fields of technology. Nowadays it can be used in the telecom sector to overcome many problems [20]. Mounted antennas can be used to extend connectivity in disaster-prone regions when terrestrial networks are in failure [2]. Even UAV's have huge contributions to provide connectivity in 5G and beyond technologies. Its high mobility makes it the best choice for mobile connectivity and aerial base station (BS) [21]. It has been predicted that the business and the market for drones will be around USD 100 billion per year by 2022. Its usage is increasing in agriculture for precision crop mapping and surveying. Recently UAV's play a huge role in the package delivery system especially for e-commerce players and it will help to overcome many problems like traffic jams, vehicular failures and late deliveries. So looking at the exponentially growing demand and market for drones makes it interesting to study and learn [11].
Growing importance of UAV's in defence sector for unmanned missions and to provide battlefield intelligence is an important aspect. So as the importance of this unmanned vehicle is increasing the study of all its components and its functions becomes important.

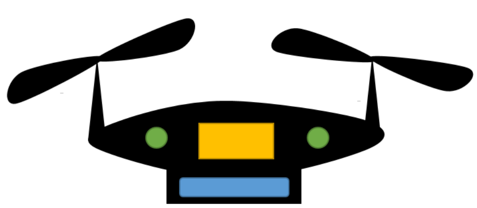

Figure 1: UAV-Unmanned Aerial Vehicles

1.2 Challenges of UAV

- The drone is a battery dependent device which makes it an energy, time and distance constrained device for high mobile requirements.
- Battery dependency decreases the range of operation.
- NLoS (non line of sight) operations are difficult to operate especially in an environment like urban and sub-urban areas.
- Energy transfer is suitable for information transfer but for power transfer it gets difficult [17].
- High mobility makes it battery consuming and draining of stored power takes place at a very fast rate.
- Energy transfer for such a highly mobile device is of utmost importance to increase the durability and range of operations [7].

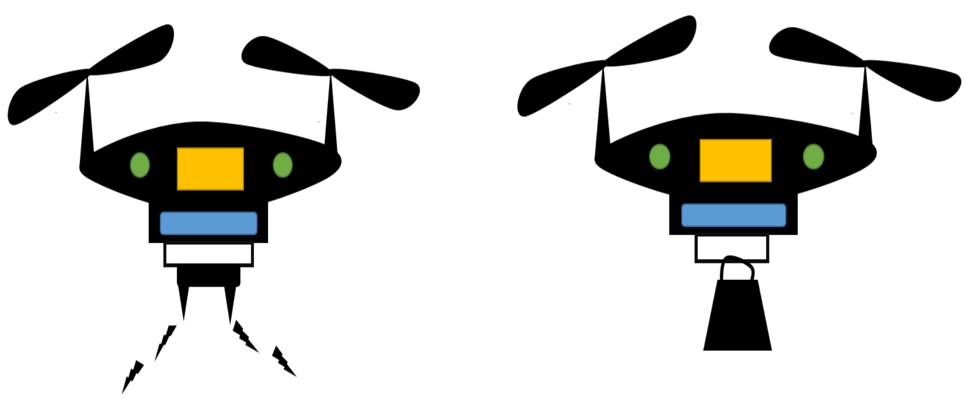

(a) UAV as transmitter

(b) UAV for package delivery

Figure 2: Uses of UAV

1.3 Intelligent Reflecting Surfaces (IRS)

IRS is a planar passive reflecting surface that is smartly able to alter phase and amplitude so that at the user end the energy and signal add up coherently and in-phase [3] [19]. These surfaces are made of electromagnetic (EM) materials which can be electronically controlled that are always helpful to deliver data and energy where line-of-sight (LOS) is difficult for communication. It makes the channel between IR and user as another line-of-sight (LOS) channel which helps to communicate even when line-of-sight (LOS) communication or energy transfer is not possible through base stations [22]. Energy and spectral efficiency make it suitable for wireless networks along with cost-effectiveness add up the advantage.
IRS is generally low-cost, lightweight and conformal geometry makes it effective for deployment and replacement. IRS makes it the best possible option especially in urban or suburban regions where LOS options are very rare [6]. IRS being a passive device always works in full-duplex mode. It is free from self-interference and antenna noise amplification. This allows us to study it's all aspects to take maximum advantage of this technology for wireless charging high mobility devices like UAVs even in non-line-of-sight (NLoS) regions [8].
In the current scenario, IRS is beneficial for the extension of the range of operation like for technology WiFi without changing any software or hardware designs or components. Along with the above advantages it can simultaneously reflect energy and information without any need of RF chains which gives an edge in SWIPT(Simultaneous wireless information and power transfer) [16].

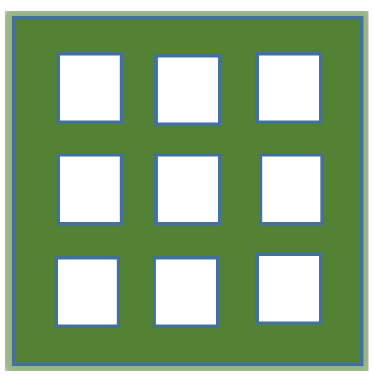

Figure 3: IRS-Intelligent Reflecting Surfaces

1.3.1 Physics of IRS [23]

The ideal case of reflection is when angle of incidence θ_i coming from a transmitter equals angle of reflection or observation angle θ_s. If anyone of these two are moving or mobile which changes angles continuously, then the main purpose of IRS is to shape the received wave in the direction of the receiver.

Consider an IRS consisting of a meta-surface of the same dimensions axb and the impinging plane wave. The intention of an IRS is to achieve ideal reflection which will point the reflected beam in a desired direction that we denote as θ_r. Hence, the surface must be designed to redirect the incident plane wave $(\mathbf{E}_i, \mathbf{H}_i)$ and obtain the following ideal field distributions of the reflected/scattered wave:

$$\mathbf{E}_r = E_r e^{-jk(\sin(\theta_r)y+\cos(\theta_r)z)} \boldsymbol{e}_x$$
$$\mathbf{H}_r = -\frac{E_r}{\eta} \left(\sin\left(\theta_r\right) \boldsymbol{e}_z - \cos\left(\theta_r\right) \boldsymbol{e}_y\right) e^{-jk(\sin(\theta_r)y+\cos(\theta_r)z)}$$

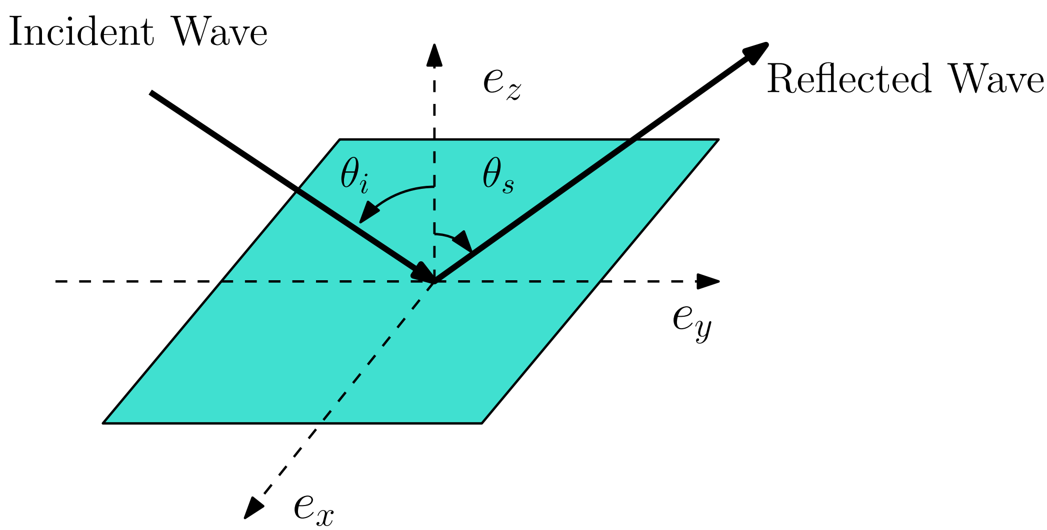

Figure 4: Wave reflection on IRS

Snell's law of reflection is a widely used approach in the literature that designs reflective meta-surfaces. Using this methodology, the required surface phase profile to transform the incident wave $(\mathbf{E}_i, \mathbf{H}_i)$ into $(\mathbf{E}_r, \mathbf{H}_r)$ is obtained by changing the surface impedance. At the surface $(z = 0)$, the superposition of the incident and reflected E-field can be written as

$$\mathbf{E}_t = E_i e^{-jk\sin(\theta_i)y}\boldsymbol{e}_x + E_r e^{-jk\sin(\theta_r)y}\boldsymbol{e}_x$$

Then, the desired phase of the desired reflection coefficient is

$$\phi_r(y) = \angle\left(\frac{E_r e^{-jk\sin(\theta_r)y}}{E_i e^{-jk\sin(\theta_i)y}}\right) = -k\sin\left(\theta_r\right)y + k\sin\left(\theta_i\right)y$$

The gradient of the reflection coefficient can be calculated by differentiating it with respect to y using generalised Snell's law:

$$k\left(\sin\left(\theta_i\right) - \sin\left(\theta_r\right)\right) = \frac{d\phi_r(y)}{dy}$$

which gives the relation between θ_i, θ_r and the local surface phase $\phi_r(y)$. By changing the surface impedance, $\phi_r(y)$ is obtained at each point of the surface and the output wave's desired phase $-k\sin\left(\theta_i\right)y + \phi_r(y) = -k\sin\left(\theta_r\right)y$ is finally achieved.

1.4 Related Literature

The authors in [1] has studied the environment parameters to compare analysis with simulation results. The authors in [2] gives an insight into the low altitude parameters and efficient way to optimise the system for optimal coverage. Importance of large intelligent surfaces for coming communication generations [3]. Multiple IRS system for communication as a key technology and coverage is formulated in [6] and [9]. The methodologies to harvest received is studied in [7]. The reports [8] and [17] studies the SWIPT technology where energy and information can be transferred simultaneously. The working of the wireless transfer of energy using massive antenna arrays was investigated in [11]. [13] has the channel loss modelling and its characterisation according to elevation angle and distance between charging station from UAV. [18] gives the formulation of equation for analysis part. To study IRS as a passive or active device and its characteristics is given in [19]. For the study of 5G and beyond technologies where IRS will play major role is given in [20]. These papers [21] and [22] relay communication along with power transfer using IRS systems. The physics ,propagation,path-loss are studied in [23].The papers [14] and [10] discuss the power splitting mechanism by which we can distribute received power between information transfer and power harvesting at the receiver end. [12] presents the practical considerations for dynamic power splitting with non-linearity of circuitry into considerations. [16] proposes the ways by which IRS can be beneficial for energy transfer when NLoS situation arises and the change in received energy with the change in IRS elements even when LoS component is present. [4] formulates the model for energy harvesting taking considerations of all non-linearity's of the practical circuit required for energy harvesting. To solve a MISO system optimization techniques such as alternating optimization is used to get the most optimal power transfer which can be studied from the paper [15].

1.5 Novel Aspects Relative to Prior Art and Our Contributions

To the best of the authors's knowledge, not much work has been done on investigating the viability of IRS-assisted WET to UAVs in terms of probability of outage under (a) comprehensive and generic channel model that accounts for path-loss, elevation angle and the probability of line-of-sight in urban or semi-urban environment and, (b) under non-linear energy harvesting model at UAVs. We first study the SISO scenario and then extend it to MISO. We also study the performance of IRS assisted wireless energy and information transfer for two different receiver architectures, namely time-splitting and power splitting. To summarize, our contributions are as follows:

- We first derive closed-form analytical expression for the probability that the received energy falls below a certain threshold at the UAV for an IRS-assisted WET in SISO(Single Input Single Output) scenario. We do this over a generic channel model that accounts for path loss, angle of elevation and probability of LoS. We then also deduce the probability of outage wherein the harvested energy goes below a certain threshold under non-linear EH at the UAV. We present results to illustrate the impact of number of IRS elements, distance between BS and UAV and the angle of elevation of UAV relative to BS on outage probability.
- We then extend out study to MISO(Multiple Input Single Output) scenario where the BS is now equipped with multiple antennas. We study performance in terms of probability of outage in WET and adopt alternating optimization to design beamforming at BS and phase-shifts at IRS such that the power received at UAV is maximized. We present results to show the impact of number of BS antennas and number of IRS elements.
- We next evaluate the performance of IRS assisted wireless energy and information transfer and highlight the trade-off for two different receiver architectures, namely time-splitting and power splitting in terms of probability of energy outage and probability of information outage.

1.6 Organisation of Thesis

- Chapter 2 discusses the energy transfer modelling and theoretical formulation from base station to UAV using IRS for a SISO (Single Input Single Output) model. This chapter also proposes the non-linear energy harvesting when non-linearity of circuit is taken into consideration and plot the outage probability for harvested power with respect to number of IRS elements and change in elevation angle.

- Chapter 3 formulates the energy transfer and energy harvesting model for MISO (Multiple Input Single Output) system. In this chapter the usage of alternating optimization is taken into consideration for optimal beam forming at the power transmitting end. It also analyses the power splitting and time splitting model taking practical non-linearity of system into consideration.

- Chapter 4 summarizes the work done and inferences drawn from this study. Some interesting avenues for future research are also discussed.

2 WET to UAV : SISO configuration

Looking at the drawbacks of a battery powered mobile devices it is important to study the ways to overcome the energy shortage during operation. This chapter discusses about the WET(Wireless energy transfer) to UAV when we consider a single BS antenna and a single UAV system. We will also try to understand the change in power received when number of IRS elements changes along with the change in distance of LoS (Line of Sight).
In this chapter, we will also observe the amount of power that will be harvested using non-linear energy harvesting model and study its changes with the change in distance and number of IRS elements.

2.1 System Model

Consider a base station situated on ground along with with IRS located at some distance away from base station. Looking at urban , sub-urban environments where tall buildings are already present. Looking at such scenario the UAV is operating at some height which needs to be charged wirelessly using direct LoS path or indirect path through IRS whenever NLoS situation arises [23]. The combination of these two paths can increase the range of charging wherever the base station is unable to charge wirelessly [9].

The fading coefficient, g_i represents small scale fading for the channel between the i th-reflecting element and UAV. f is the direct channel small scale fading coefficient and the small scale fading coefficient h_i for channel between BS and ith-reflecting element (RE).All the above small scale fading are considered as $C\mathcal{N}(0,1)$ i.e. $h_i \sim C\mathcal{N}(0,1)$,
$g_i \sim C\mathcal{N}(0,1)$ and $f \sim C\mathcal{N}(0,1)$.
The direct path signal received by the UAV is given by [13],

$$r_1 = \left[\sum_{i=1}^{N} h_i \sqrt{L_{BS,i}^{-1}} e^{j\psi_i} g_i \sqrt{L_{UAV,i}^{-1}}\right] x \tag{1}$$

The received signal due to indirect path is given by,

$$r_2 = \left[f \sqrt{L_{DIR}^{-1}}\right] x \tag{2}$$

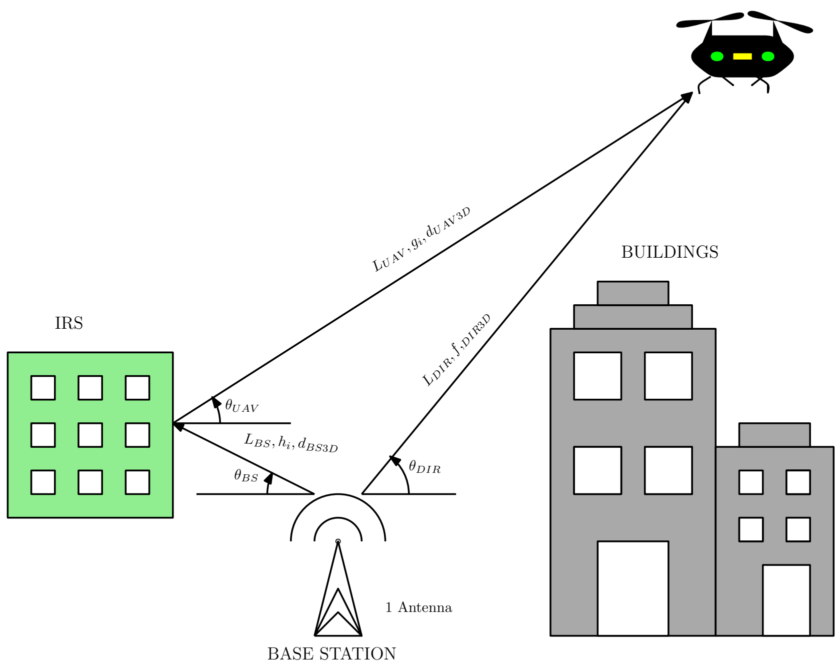

Figure 5: SISO system model

here, $L_{BS,i}$ is the path loss between the base station and the ith-reflecting element, $L_{UAV,i}$ represents the path loss between the i th-reflecting element present on IRS and UAV. L_{DIR} stands for the path loss for the path from base station to the UAV. N represents number of reflecting elements present in the IRS, where each reflecting element changes a phase shift ψ_i of the reflected wave independently. Channels characteristics in terms of their envelopes and phases can be written as $h_i = \alpha_i e^{-j\omega_i}$, $g_i = \beta_i e^{-j\emptyset_i}$ and $f = \gamma e^{-j\theta}$.
Assuming the IRS has prior information of channel state information (CSI), the phase shifts changed by IRS elements can be selected to cancelout the channel phases as $\psi_i = \omega_i + \emptyset_i - \theta$. α_i, symbolize the envelope of the channel the BS to i th-RE in the IRS, which is generally considered as Rayleigh distribution because it takes into consideration the multipath fading which is caused by by multi-path transmission. It forms a realistic settings for simulation purposes. With the similar perspective and realistic approach, the envelopes of the channels between the ith-reflecting element in the IRS and the UAV (β_i) and direct path from BS to UAV (γ) is also taken as Rayleigh distribution. E_s is the transmitted energy from BS.

So, the energy received is given by,

$$E_{rxed} = | \left[\sqrt{L_1} \sum_{i=1}^{N} |\alpha_i||\beta_i| \right] + \left[|f| \sqrt{L_2} \right] |^2 E_s \tag{3}$$

$$E_{rxed} = [L_1 \left| \sum_{i=1}^{N} |\alpha_i||\beta_i| \right|^2 + |f|^2 L_2 + 2 \left| \sqrt{L_1} \sum_{i=1}^{N} |\alpha_i||\beta_i| \right| \left| |\gamma| \sqrt{L_2} \right|] E_s \tag{4}$$

where $L_1 = L_{BS}^{-1} L_{UAV}^{-1}$ and $L_2 = L_{DIR}^{-1}$.

The direct channel path loss from BS to UAV is based on two major factors, the elevation angle (θ_{DIR}) and the 3D distance from the BS to the UAV (d_{DIR3D}) . The path loss between the IRS and the BS (L_{BS}) is also based on the above two factors (θ_{BS}) and the 3D distance (d_{BS3D}). Similarly,(L_{UAV}) the path loss between the IRS and the UAV is based on the elevation angle (θ_{UAV}) and 3D distance (d_{UAV3D}). The angle-dependent and 3D distance path loss models always fit better in experimental path loss modeling [13].

$$\begin{aligned} L_{\mathrm{UAV}}^{\mathrm{dB}} (\theta_{\mathrm{UAV}}, d_{\mathrm{UAV3D}}) = & \left(L_{\mathrm{FS}}^{\mathrm{dB}} (d_{UAV3D}, f) + \eta_{\mathrm{NLOS}} \right) (1 - P_{\mathrm{LOSUAV}} (\theta_{\mathrm{UAV}})) \\ & + \left(L_{\mathrm{FS}}^{\mathrm{dB}} (d_{\mathrm{UAV3D}}, f) + \eta_{\mathrm{LOS}} \right) P_{\mathrm{LOSUAV}} \ (\theta_{\mathrm{UAV}}) , \end{aligned} \tag{5}$$

where $P_{\mathrm{LOSUAV}} (\theta_{\mathrm{UAV}}) = \frac{1}{1 + a_{UAV} e^{-b_{UAV} (\theta_{UAV} - a_{UAV})}}$.

The P_{LOSUAV} represents the LoS probability between the UAV and the IRS, which depends on the elevation angle (θ_{UAV}), and $L_{\mathrm{FS}} (d_{UAV3D}, f)$ is the free-space path loss as a function of distance and frequency. The parameters b_{UAV} and a_{UAV} are discrete to the surrounding which we trying to study such as urban, suburban, etc. These parameters can be calculated from Tables I-II [1]. Therefore, L_{UAV} (θ_{UAV} , d_{UAV3D}) has a LoS and a non line-of-sight (NLoS) components that are combined based on $P_{\mathrm{LOS}} (\theta_{UAV})$ that takes into account the UAV channels.

The path loss (in decibels) is given as,

$$\begin{aligned} L_{\mathrm{UAV}}^{\mathrm{dB}} (\theta_{\mathrm{UAV}}, d_{\mathrm{UAV3D}}) = & (\eta_{\mathrm{LOS}} - \eta_{\mathrm{NLOS}}) P_{\mathrm{LOSUAV}} (\theta_{\mathrm{UAV}}) \\ & + 20 \log \left(d_{\mathrm{UAV3D}} \frac{4\pi}{\lambda} \right) + \eta_{\mathrm{NLOS}} \end{aligned} \tag{6}$$

In (6), η_{LOS} and η_{NLOS} symbolize the excess path loss along with the free-space path loss for both LoS and NLoS respectively. Similarly, b_{BS}, a_{BS}, b_{DIR}, a_{DIR} are specified for the surroundings used for study such as urban, suburban, etc. These can be calculated from the Tables I-II [1].
The received energy at the IRS, P_r, and the path loss, $L_{\text{BS}}^{\text{dB}}$, between BS and the UAV, taking sidelobe of the BS and 3-D distance into consideration can be written as [13],

$$P_r = P_T \eta_\nu G_{sl} H_\nu d_{BS3D}^{-\kappa_\nu}, \quad \nu \in \{\text{LoS}, \text{NLoS}\} \tag{7}$$

and

$$\begin{aligned} L_{\text{BS}}^{\text{dB}}(\theta_{\text{BS}}, d_{\text{BS3D}}) = &\left(10\kappa_{NLOS}\log(d_{BS3D}) + \eta_{\text{NLOS}}\right)(1 - P_{\text{LOSBS}}(\theta_{\text{BS}})) \\ &+ \left(10\kappa_{LOS}\log(d_{BS3D}) + \eta_{\text{LOS}}\right)P_{\text{LOSBS}}(\theta_{\text{BS}}) - G_{sl} \\ &+ 20\log\left(\frac{4\pi}{\lambda}\right) \end{aligned} \tag{8}$$

where, $P_{\text{LOSBS}}(\theta_{\text{BS}}) = -a_{BS}e^{-b_{BS}.\theta_{\text{BS}}} + c_{BS}$

Similarly,the path loss $L_{\text{DIR}}^{\text{dB}}$ between BS and UAV is given by [13],

$$\begin{aligned} L_{\text{DIR}}^{\text{dB}}(\theta_{\text{DIR}}, d_{\text{DIR3D}}) = &\left(10\kappa_{NLOS}\log(d_{DIR3D}) + \eta_{\text{NLOS}}\right)(1 - P_{\text{LOSDIR}}(\theta_{\text{DIR}})) \\ &+ \left(10\kappa_{LOS}\log(d_{DIR3D}) + \eta_{\text{LOS}}\right)P_{\text{LOSDIR}}(\theta_{\text{DIR}}) \\ &- G_{sl} + 20\log\left(\frac{4\pi}{\lambda}\right) \end{aligned} \tag{9}$$

where, $P_{\text{LOSDIR}}(\theta_{\text{DIR}}) = -a_{DIR}e^{-b_{DIR}\theta_{\text{DIR}}} + c_{DIR}$.

To covert the calculated channel losses in decibels to linear scale we use,

1. $L_{\text{DIR}} = 10^{-L_{\text{DIR}}^{\text{dB}}/10}$ - channel loss between BS antennas and UAV.
2. $L_{\text{UAV}} = 10^{-L_{\text{UAV}}^{\text{dB}}/10}$ - channel loss between IRS and UAV.
3. $L_{\text{BS}} = 10^{-L_{\text{BS}}^{\text{dB}}/10}$ - channel loss between BS antennas and IRS.

2.2 Analysis for received energy outage probability

Total energy received is [18],

$$E_{rxed} = |\left[\sqrt{L_1}\sum_{i=1}^{N}|\alpha_i||\beta_i|\right] + \left[|\gamma|\sqrt{L_2}\right]|^2 E_s \tag{10}$$

Let,

$$X_1 = \sum_{i=1}^{N}|\alpha_i||\beta_i|$$

$$Y_1 = |\gamma|$$

The PDF of X_1 and Y_1 can be written as

$$f_{X_1}(x) = \frac{1}{\sqrt{2\pi\sigma^2}}e^{-\frac{(x-s)^2}{2\sigma^2}}, f_{Y_1}(y) = \frac{y}{\lambda_D}e^{-\frac{y^2}{2\lambda_D}}$$

According to the Central Limit Theorem (CLT), X_1 is approximately modeled as a Gaussian random variable with mean $s = \frac{N\pi}{4}$ and variance as $\sigma^2 = N\left(1 - \frac{\pi^2}{16}\right)$. Similarly, $Y_1 = |h_D|$ can be approximated as a Rayleigh-distributed random variable with parameter $\lambda_D = \frac{1}{2}$.
We get,

$$E_T = \left|\sqrt{L_1}X_1 + \sqrt{L_2}Y_1\right|^2 E_s \tag{11}$$

Suppose,

$$K_1 = L_1 E_s$$

$$K_2 = L_2 E_s$$

We get,

$$E_T = \left|\sqrt{K_1}X_1 + \sqrt{K_2}Y_1\right|^2 \tag{12}$$

$$Z^2 = \left|\sqrt{K_1}X_1 + \sqrt{K_2}Y_1\right|^2 \tag{13}$$

$$Z = \left|\sqrt{K_1}X_1 + \sqrt{K_2}Y_1\right| \tag{14}$$

$$F_Z(z) = Pr(\sqrt{K_1}X_1 + \sqrt{K_2}Y_1 < z) \tag{15}$$

The CDF of F_{Ethrs} is given by [18],

$$\begin{aligned} F_Z(z) =& 1/2[erf((az/p-s)/\sqrt{2\sigma^2}) + erf(s/\sqrt{2\sigma^2}] \\ & - 1/2(\sqrt{\lambda_d}/c_1)exp^{-(az-ps)^2/2c_1^2} erf((c_4z-c_5)/c_1c_2) \\ & - 1/2(\sqrt{\lambda_d}/c_1)exp^{-(az-ps)^2/2c_1^2} erf((c_3z+c_5)/c_1c_2) \end{aligned} \tag{16}$$

where, $c_1 = \sqrt{\sigma^2 p^2 + \lambda_D}$, $c_2 = \sqrt{2\sigma^2\lambda_D}$, $c_3 = \sigma^2 ap$, $c_4 = \lambda_D a/p$

$c_5 = \lambda_D s$, $a = 1/\sqrt{K_1}$, $p = \sqrt{K_1/K_2}$

Suppose, $J_1 = 1/2(erf((az/p-s)/\sqrt{2\sigma^2}) + erf(s/\sqrt{2\sigma^2}))$

$$\begin{aligned} J_2 =& 1/2(\sqrt{\lambda_d}/c_1)exp^{-(az-ps)^2/2c_1^2} erf((c_4z-c_5)/c_1c_2) \\ & + 1/2(\sqrt{\lambda_d}/c_1)exp^{-(az-ps)^2/2c_1^2} erf((c_3z+c_5)/c_1c_2) \end{aligned} \tag{17}$$

Then we get,

$$F_Z(z) = J_1 - J_2 \tag{18}$$

Thus we can obtain CDF of Z^2 as [18],

$$F_{Z^2}(t) = F_Z(\sqrt{t}) \tag{19}$$

The outage probability is given as,

$$\begin{aligned} P_{outage} =& \frac{1}{2}\left(\text{erf}\left(\frac{a/\rho\sqrt{E_{thrs}} - s}{\sqrt{2\sigma^2}}\right) + \text{erf}\left(\frac{s}{\sqrt{2\sigma^2}}\right)\right) \\ & - \frac{1}{2}\frac{\sqrt{\lambda_D}}{c_1} e^{\left(-\frac{(a\sqrt{E_{thrs}}-\rho s)^2}{2c_1^2}\right)} \text{erf}\left(\frac{c_4\sqrt{E_{thrs}} - c_5}{c_1c_2}\right) \\ & - \frac{1}{2}\frac{\sqrt{\lambda_D}}{c_1} e^{\left(-\frac{(a\sqrt{E_{thrs}}-\rho s)^2}{2c_1^2}\right)} \text{erf}\left(\frac{c_3\sqrt{E_{thrs}} + c_5}{c_1c_2}\right) \end{aligned} \tag{20}$$

2.3 Non-linear energy harvesting model

Wireless energy transfer is a promising solution to increase durability and range of UAV to complete many tasks.Along with energy transfer, energy harvesting is also an important perspective to harvest the received energy and store it in battery for further usage.So for this energy harvesting (EH) circuits comes into picture. These circuits harvest received energy into stored energy. But to model this conversion earlier liner model were used but it was not accurate and were not according to practical perspective. So as to overcome this problem non-linear energy harvesting model is used which is almost close to that of practical EH circuits. Such models gives us clear picture about the range of energy/power will be stored in the battery [4]. For low power circuits energy conversion efficiency is more with more input power and vice versa. Along with this there are limitations regarding the maximum amount of energy that can be harvested. The following model is accurate only when all the parameters and variables of EH circuits remains constant.

$$\tau_{\mathrm{ER}_j}^{\mathrm{Practical}} = \frac{\left[\chi_{\mathrm{ER}_j}^{\mathrm{Practical}} - M_j\Lambda_j\right]}{1-\Lambda_j} \tag{21}$$

$$\Lambda_j = \frac{1}{1+\exp\left(a_j b_j\right)} \tag{22}$$

$\tau_{\mathrm{ER}_j}^{\mathrm{Practical}}$ is the total harvested energy at the receiving end and Λ_j is to ensure the zero-input zero-output response of the EH circuit.

$$\chi_{\mathrm{ER}_j}^{\mathrm{Practical}} = \frac{M_j}{1+\exp\left(-a_j\left(P_{\mathrm{ER}_j}-b_j\right)\right)} \tag{23}$$

In the above equation, χ_{ER_j} is the logistic function w.r.t.received RF power ER_j. $a_j$and b_j are the constants related to the circuit specifications such as turn-on voltage , resistance and capacitance. M_j is the maximum energy harvested by the given EH circuit [4]. The values of $a_j = 6400$, $b_j = 0.003$ and $M_j = 20mW$.

2.3.1 Outage probability for harvested power

To find the outage probability w.r.t harvested power we will compare harvested power with threshold. Firstly we will find harvested power as,

$$\tau_{\mathrm{ER}_j}^{\text{Practical}} = \frac{\left[\chi_{\mathrm{ER}_j}^{\text{Practical}} - M_j\Lambda_j\right]}{1-\Lambda_j} \tag{24}$$

$$\Lambda_j = \frac{1}{1+\exp\left(a_j b_j\right)} \tag{25}$$

So, $\Lambda_j = \frac{1}{1+\exp(6400*0.003)} = 4.5871*10^{-9}$.

$\tau_{\mathrm{ER}_j}^{\text{Practical}}$ is the total harvested energy at the receiving end and Λ_j is to ensure the zero-input zero-output response of the EH circuit.

$$\chi_{\mathrm{ER}_j}^{\text{Practical}} = \frac{M_j}{1+\exp\left(-a_j\left(P_{\mathrm{ER}_j}-b_j\right)\right)} \tag{26}$$

The values of $a_j = 6400$, $b_j = 0.003$ and $M_j = 20mW$.
As, $\Lambda_j << 1$ and $1-\Lambda_j \approx 1$.

So the equation now becomes, $\tau_{\mathrm{ER}_j}^{\text{Practical}} = \chi_{\mathrm{ER}_j}^{\text{Practical}} - M_j\Lambda_j$.

To find outage probability, $P_{out} = Pr(\tau_{\mathrm{ER}_j}^{\text{Practical}} < E_{thrs})$.

$$P_{out} = Pr(\chi_{\mathrm{ER}_j}^{\text{Practical}} - M_j\Lambda_j < E_{thrs}) \tag{27}$$

$$\begin{aligned}
Pr(\chi_{\mathrm{ER}_j}^{\text{Practical}} - M_j\Lambda_j < E_{thrs}) &= Pr(\chi_{\mathrm{ER}_j}^{\text{Practical}} < E_{thrs} + M_j\Lambda_j) \\
&= Pr\left(\frac{M_j}{1+\exp\left(-a_j\left(P_{\mathrm{ER}_j}-b_j\right)\right)} < E_{thrs} + M_j\Lambda_j\right) \\
&= Pr\left(\exp\left(-a_j\left(P_{\mathrm{ER}_j}-b_j\right)\right) < \frac{M_j}{E_{thrs}+M_j\Lambda_j} - 1\right) \\
&= Pr\left(\left(-a_j\left(P_{\mathrm{ER}_j}-b_j\right)\right) < ln\left(\frac{M_j}{E_{thrs}+M_j\Lambda_j} - 1\right)\right) \\
&= Pr\left(P_{\mathrm{ER}_j} < \frac{-1}{a_j} ln\left(\frac{M_j}{E_{thrs}+M_j\Lambda_j} - 1\right) + b_j\right)
\end{aligned}$$

2.4 Simulation Results

To understand the variation of received power and harvested power at UAV w.r.t increase in number of IRS elements and also with change in the elevation angle w.r.t BS.

Simulation parameters for received power [13]:- .

Category	Value
Propagation environment	Suburban
Frequency	700MHz
$(\eta_{\text{Los}}, \eta_{\text{NLOS}})$	$(0, 18)$dB
$(\kappa_{\text{Los}}, \kappa_{\text{NLOS}})$	$(2.5, 3.5)$
$(a_{\text{gUE}}, b_{\text{gUE}})$	$(4.88, 0.4472)$
$(a_{\text{BS}}, b_{BS}, c_{\text{BS}})$	$(1, 6.581, 1)$
G_{s1}	-15 dB
Transmitted power	1W
Received power threshold for P_{out}	2x$10^{-5}W$

For non-linear energy harvesting simulation parameters are [4]:-

Category	Value
Propagation environment	Suburban
Frequency	700MHz
a_j	6400
b_j	0.003
M_j	20mW
Transmitted power	1W
Harvested power threshold for P_{out}	2x$10^{-12}W$

2.4.1 Plots between number of IRS elements and outage probability for received power

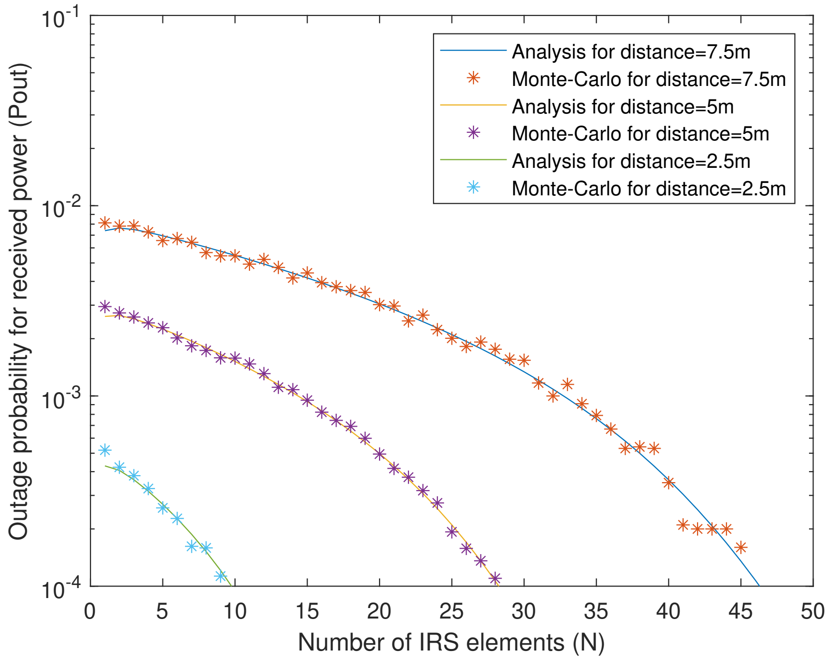

Figure 6: Change in Outage probability(Pout) with the change in number of IRS elements(N). Elevation angle between UAV and BS $=25^o$

The above plot proves that, the increase in distance between base station(BS) and UAV leads to increases in the outage probability for the same number of IRS elements. To get the same outage probability for larger distances we require more number of IRS elements for the same amount of transmitted energy.

2.4.2 Plot between elevation angle and outage probability for received power

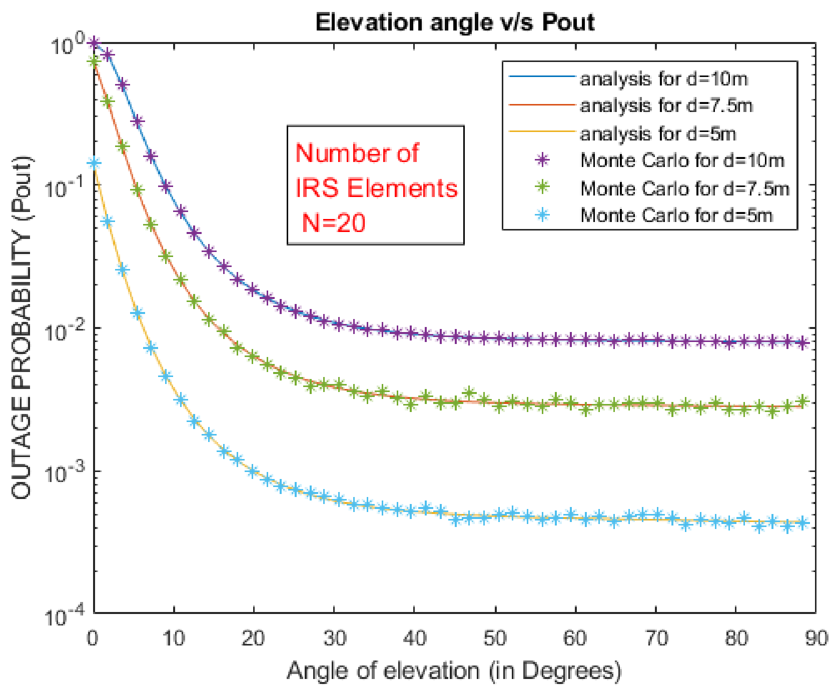

Figure 7: Change in outage probability with the change in elevation angle between UAV and BS. Number of IRS elements =20

The above plot gives insight on how the outage probability varies w.r.t elevation angle for the same number of IRS. For same number of IRS elements as the angle of elevation decreases w.r.t. base station the outage probability also increases as probability of LoS also decreases with decrease in elevation angle. This plot also shows that as the distance between BS and UAV increases the outage probability for received power decreases when the elevation angle between BS and UAV is constant.
This proves that, as distance of operation decreases and elevation angle increases the overall performance of the system and power transfer increases.

2.4.3 Number of IRS elements v/s outage probability for Non-linear energy harvesting

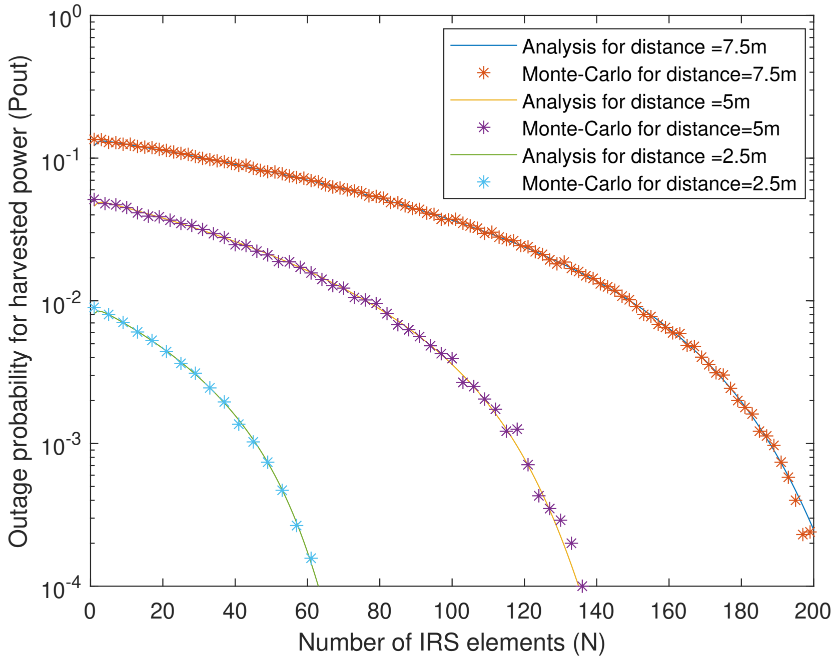

Figure 8: Impact of change in No.of IRS elements on outage probability (Pout). Elevation angle between UAV and BS = 25^o

In the above plot, the outage probability decreases with the increase in number of IRS elements as the harvested power increases with the increase in IRS elements when the distance between BS to UAV is constant.
As the distance increases, the outage probability increases for the same number of IRS elements. From the above plot, it can be concluded that less distance and more number of IRS elements is the good combination to decrease outage probability.

2.4.4 Elevation angle v/s outage probability for Non-linear energy harvesting

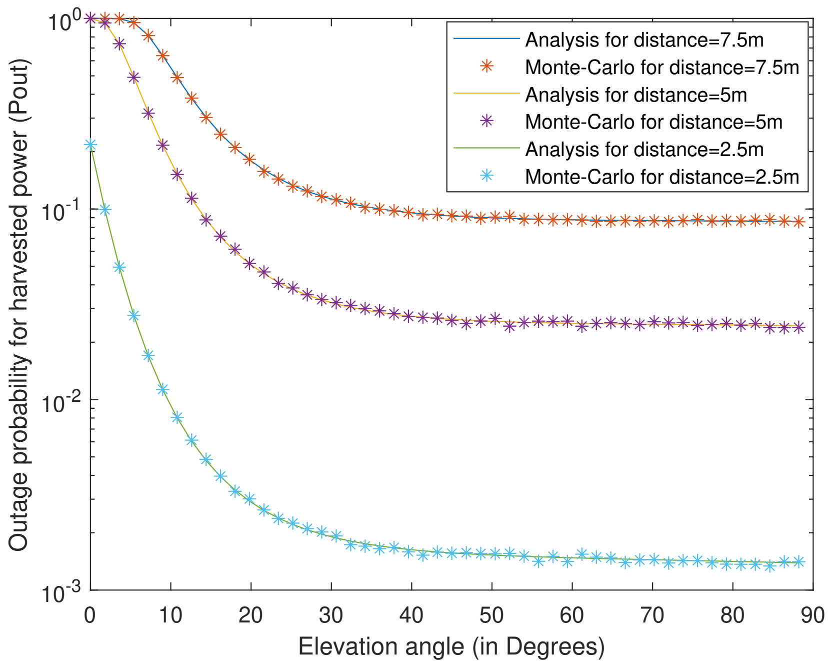

Figure 9: Impact of change in elevation angle on outage probability (Pout). Number of IRS elements (N)= 20

From the above plot, it can be concluded that the outage probability decreases with the increase in elevation angle. As the elevation angle of UAV increases the UAV comes in more LoS of BS antennas so the energy transfer becomes more efficient.
After 30^o the UAV has a LoS path for power transfer and LoS path becomes major contributor for power transfer which leads to constant outage probability after 30^o of elevation angle.
Even as the distance increases the outage probability increases as the energy transfer gets hampered exponentially which decreases the harvested power with the increase in distance.

2.5 Summary

In this chapter we have studied the WET in a SISO model. It gives an insight about the variation of received and harvested power with the change in number of IRS and distance between BS to UAV. Non-linear energy harvesting model gives more practical insight about the amount of power will be harvested from received power when non-linear circuitry comes into picture. From the above chapter it can be concluded that :-

1. The power transfer increases with the increase in elevation angle and increase in number of IRS elements with range of operation to be at lesser distance.

2. The performance of the system decreases when the CSI (Chanel state information) is unknown to the BS.

3. To verify our results they are compared with the analytical results which shows exact overlapping, proves that our model works perfectly fine even after considering practical parameters.

3 WET to UAV : MISO configuration

In the previous chapter we discussed the power transfer and harvesting keeping only one BS antenna at the base station. Now in this chapter we will observe the variation in power transfer to the UAV by changing the single antenna at the base station to multiple antennas at the base station along with the changes in elevation angle, number of IRS elements and distance between BS and UAV.

3.1 System Model

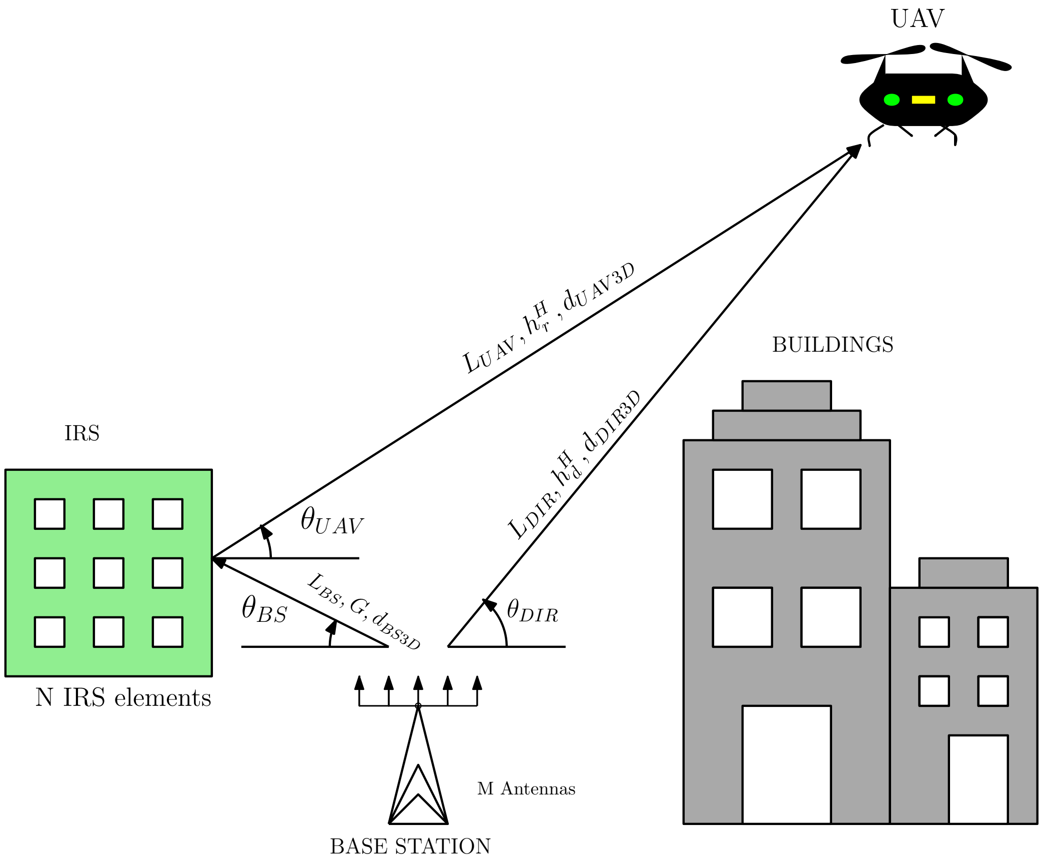

Figure 10: MISO System Model

Consider a base station(BS) with multiple antennas and IRS located at some distance from base station(BS) with N number of IRS elements. An UAV is located at some height operating in urban or semi-urban settlements. So it basically forms MISO system where multiple BS antennas are trying to charge using direct and indirect path.In direct path multiple BS antennas have LoS energy propagation of energy whereas in indirect path energy has to travel BS-IRS-UAV. These two paths helps to increase the range of operation as range of wireless charging even when the UAV is not in LoS with the BS. In MISO model, we have multiple direct i.e. BS-UAV and indirect paths i.e. BS-IRS and IRS-UAV which are denoted as $h_d^H \epsilon C^{1\times M}$, $G \epsilon C^{N\times M}$ and $h_r^H \epsilon C^{1\times N}$ respectively. For the above model we consider transmit beamforming at the BS which is denoted by $v \epsilon C^{Mx1}$, where $||v||^2 \leq P$ ($||.||$ denotes Euclidean norm of complex vector).
The total signal received at the user is given as,

$$P_T = (h_r^H \Theta G + h_d^H)vx + n \tag{28}$$

In the above equation x denotes i.i.d (independent and identically distributed) random variable with unit variance and zero mean, n denotes AWGN (Additive White Gaussian Noise).
Total signal power received by the UAV from both, direct and indirect channels is given by,

$$P_T = |(h_r^H \Theta G + h_d^H)v|^2 \tag{29}$$

To implement the above equation, Distributed Algorithm is used which is a low complexity algorithm where BS beam forming is iteratively optimized with the phases of IRS elements. In the above optimization one is fixed and another is adjusted for a number of times until in-phase addition does take place at UAV. This method helps to minimize the phase difference between direct and indirect path energy components.

3.2 Alternating Optimization

This is a low complexity algorithm based on alternating optimization. The beamforming at the BS is optimized alternatively with the phases of the IRS elements. In each iteration one parameter is fixed and another is varied until both are converged to the best possible combinations. To maximize the harvested power, the objective function is to be maximized [15].

The objective function is,

$$\begin{aligned} max\ |(h_r^H \Theta G + h_d^H)v|^2 \\ s.t.\ ||v||^2 \leq P, \\ 0 \leq \theta_n \leq 2\pi,\ \forall n = 1, ..., N \end{aligned} \tag{30}$$

To maximize objective function we need to maximize,

$$|(h_r^H \Theta G + h_d^H)v| = |h_r^H \Theta G v + h_d^H v| \leq |h_r^H \Theta G v| + |h_d^H v| \tag{31}$$

To hold the equality in above case and using change of variable,
$\arg(h_r^H \Theta G v) = \arg(h_d^H v) = \varphi \quad and \quad (h_r^H \Theta G v) = u^H a.$
where, $u = [e^{j\theta_1}, ...e^{j\theta_N}]^H$ and $a = diag(h_r^H)Gv.$

As, $|h_d^H v|$ is a constant term so it can be ignored in optimization.Now the optimization part is reduced to,

$$\begin{aligned} \max_u\ |u^H a| \\ s.t.\ |u_n| = 1, \quad \forall n = 1, ..., N \\ arg(u^H a) = \varphi \end{aligned} \tag{32}$$

The solution for above problem is,

$$\theta^* = \varphi - arg(h_{n,r}^H g_n^H v) = \varphi - arg(h_{n,r}^H) - arg(g_n^H v) \tag{33}$$

where, $h_{n,r}^H$ is the nth element of h_r^H and g_n^H is the nth row vector of G. For a given θ the transmit beam forming is optimized to

$$v_{MRT} = \sqrt{P} \frac{(h_r^H \Theta G + h_d^H)^H}{||(h_r^H \Theta G + h_d^H)||} \tag{34}$$

As v_{MRT} different for different iterations, so the phase change would always remain there without changing magnitude. So transmit beamforming is modified as,

$$v^* = \sqrt{P} \frac{(h_r^H \Theta G + h_d^H)^H}{||(h_r^H \Theta G + h_d^H)||} e^{j\alpha} \tag{35}$$

3.3 Distributed Algorithm

To practically implement the above Alternating Optimization, the Distributed Algorithm is developed which is a low complexity methodology [15]. This Distributed Algorithm can be implemented in a step-by-step manner as given below [5].

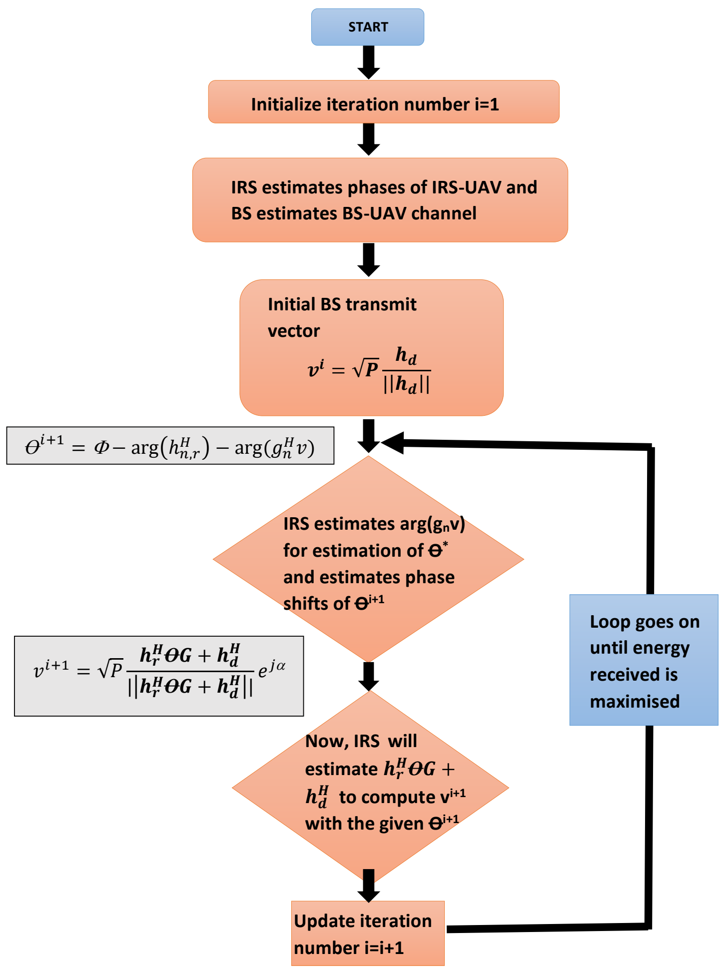

Figure 11: Distributed Algorithm

3.4 Simulation Results for MISO model

3.4.1 Average Received Power v/s number of IRS elements and number of BS antennas

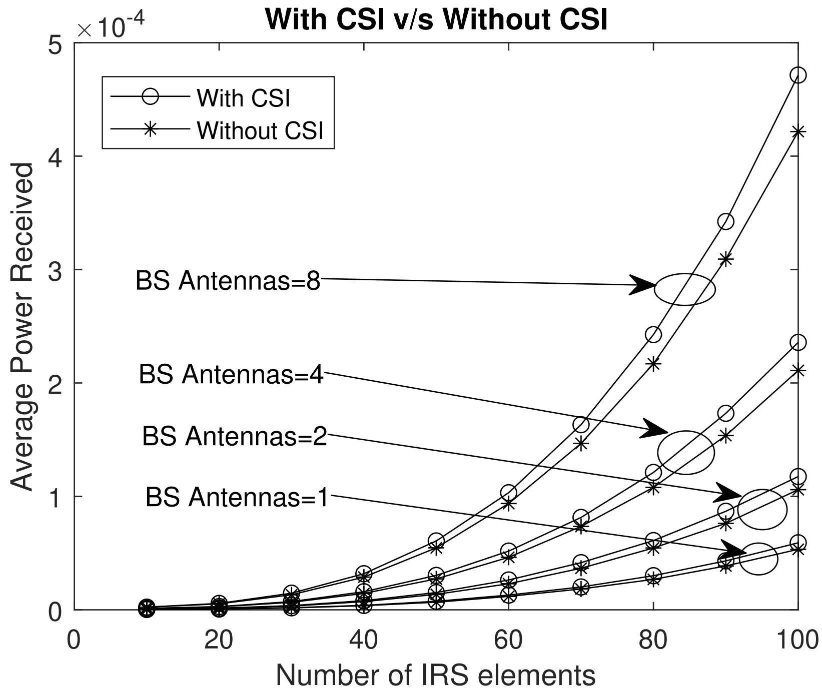

Figure 12: Average power received for different no. of BS antennas.
The distance between BS to UAV= 5m and elevation angle= 25^o.

In the above figure, the average power received is increasing with the increase in number of IRS elements. For the same number of IRS elements average power received is increasing with the increase in number of BS antennas.The average power received when the CSI is known at BS antennas is more in comparison with when the CSI is not known to BS.
So as to increase the overall performance of the system there should be balance between the the total power received in comparison with the total power consumed by the BS antennas.

3.4.2 Harvested power v/s BS antennas and number of IRS elements

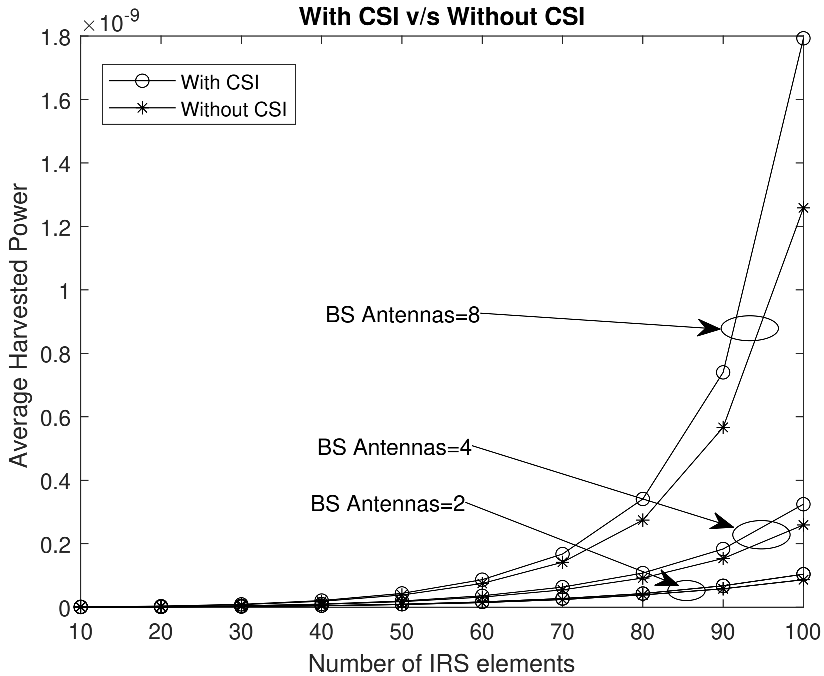

Figure 13: Average power harvested at UAV for different no. of BS antennas. The distance between BS to UAV= 5m and elevation angle= 25^o.

Using the non-linear energy harvesting model, the average power harvested is increasing with the increase in number of IRS elements. For the same number of IRS elements average power harvested is increasing with the increase in number of BS antennas.The average power received when the CSI is known at BS antennas is more in comparison with when the CSI is not known to BS antennas.

So as to increase the overall performance of the system there should be balance between the the total power harvested in comparison with the total power consumed by the BS antennas.

3.5 Outage Probability for harvested power

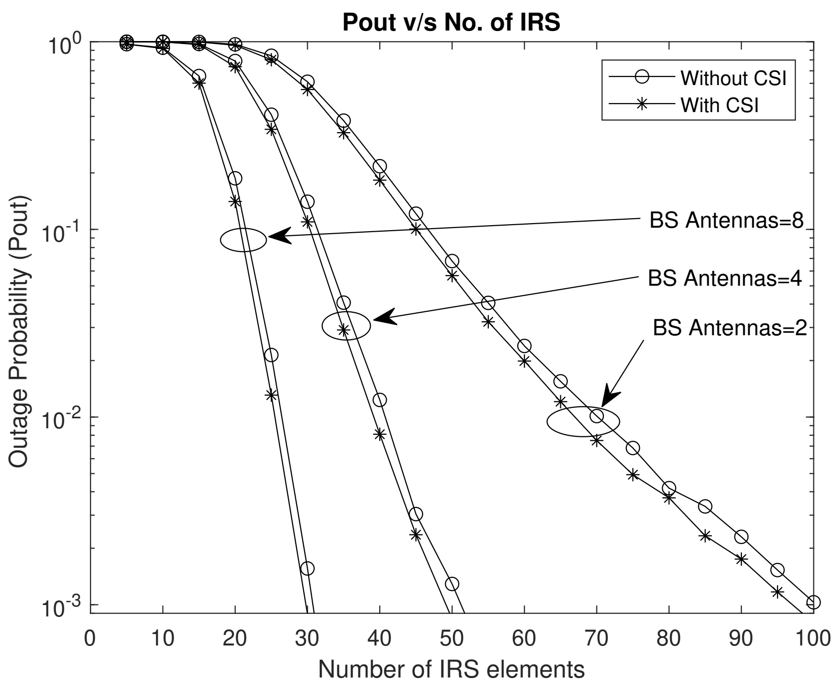

Figure 14: Impact on outage probability(Pout) with the change in number of IRS elements(N). The distance between BS to UAV= 5m and elevation angle= 25^o.

From the above figure, we conclude that the outage probability decreases with the increase in number of IRS elements. As the number of BS antennas increases the outage probability for harvested power also decreases. The performance of overall system decreases when CSI is not known to BS as compared to when CSI is known to BS when the number of IRS elements are constant.

3.6 Receive Architecture

As the need of power is increasing for energy consuming devices because of sensors, transmitting antennas and receptive antennas. The need has arrived to study the architecture by which both energy can be harvested along with it information transfer can also take place.To devise a mechanism there are two possibilities:-
1)Limited power transfer.
2)Power transmitted for a limited time (T).
In the first case, the total received power can be distributed into 2 parts depending upon the splitting factor(λ). The λ portion of the received power will be harvested whereas the remaining portion i.e. $1 - \lambda$ portion will be utilised by the UAV for information transfer.

Whereas, in the second case if the power is transmitted for a limited time duration where time distribution for energy harvesting and information transfer depends upon the time splitting factor(τ). The time portion τ will be dedicated only for power harvesting and the remaining portion (1-τ) will be utilised for information transfer when we have limited time for power transfer to the UAV.

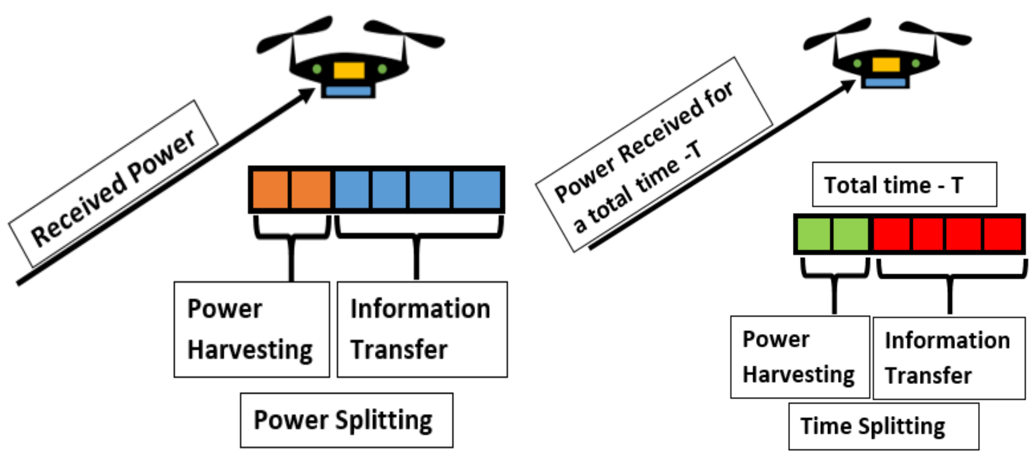

(a) Power Splitting (b) Time Splitting

Figure 15: Receive Architecture

3.6.1 Power Splitting

As the need of energy and data transfers is increasing, the demand for wireless energy and data transfer is also increasing [12]. So the demand for SWIPT(Simultaneous wireless information and power transfer) technologies are increasing [14]. The case in which a user or sensor node i.e. UAV (in our case) is sending some information or data for data acquisition of a region then the requirement for UAV is only power for its working and data transfer.In such cases the dynamic power allocation technique work where received power is distributed among data transfer and energy harvesting [10].

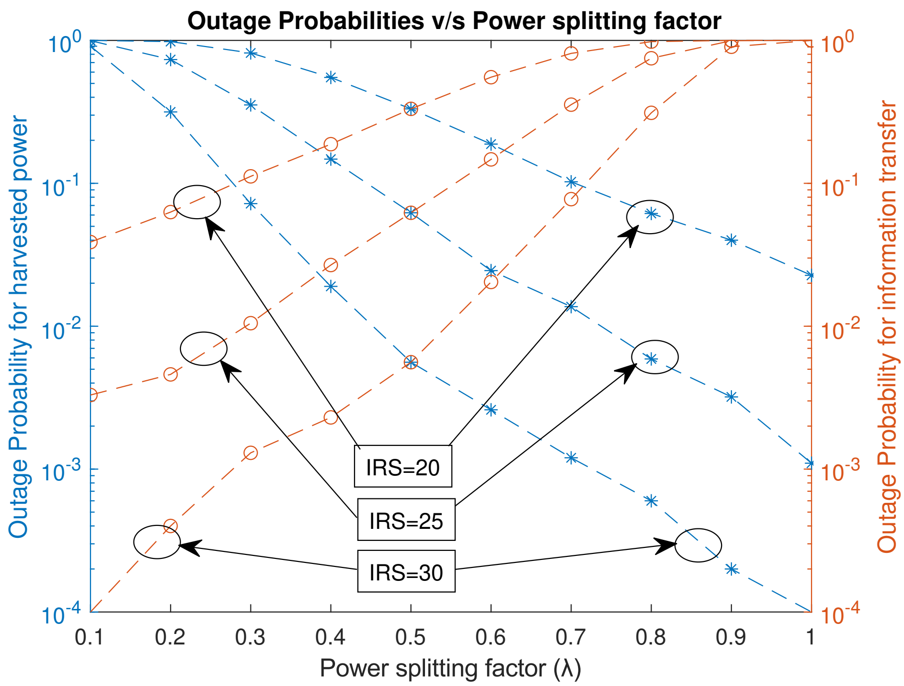

Figure 16: Change in outage probabilities for power harvesting and information transfer for change in power splitting factor. Distance between BS to UAV=5m and elevation angle=25^o

The above plot shows that as the fraction of power harvesting increases the outage probability of information transfer increases and outage probability of harvested power decreases.The outage probability for each case decreases with increase in IRS elements.

3.6.2 Time Splitting

As the above case, if the limited time is provided for energy transfer then time splitting becomes an important thing to discuss. So the time must splitting for power harvesting and information transfer becomes important to study.

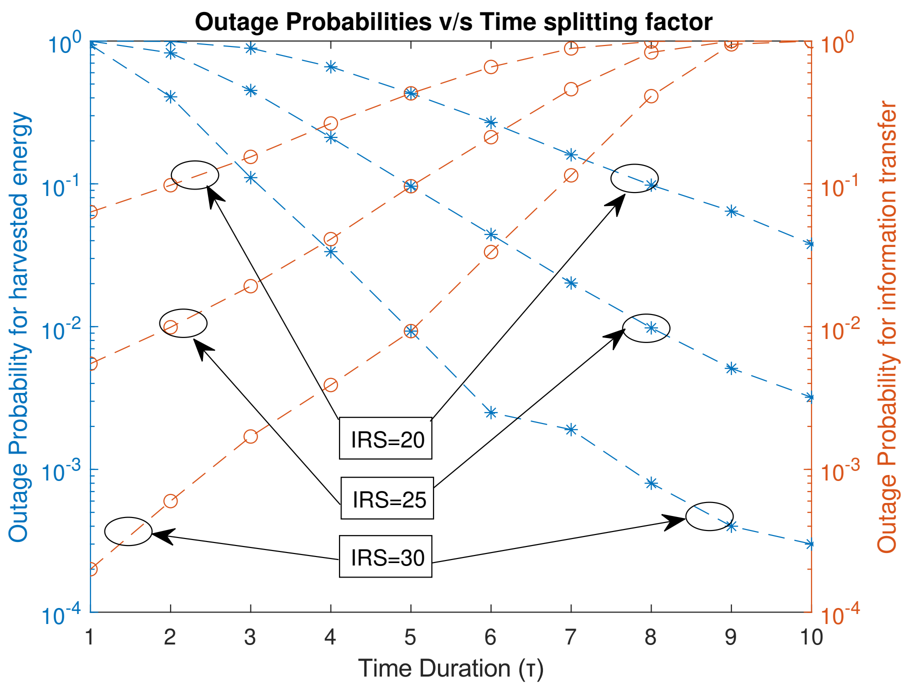

Figure 17: Change in outage probabilities for power harvesting and information transfer for change in power splitting factor. Distance between BS to UAV=5m and elevation angle=25^o

The plot proves that, as the time duration for power harvesting increases the outage probability for information transfer increases and outage probability for harvested power decreases. As the number of IRS elements increases the outage probability decreases for each case.

3.7 Summary

In this chapter we have studied the WET in a MISO model. It gives an insight about the variation of received and harvested power with the change in number of IRS, distance between BS to UAV and number of antennas at the BS. Non-linear energy harvesting model gives more practical scenario about the amount of power will be harvested from received power when non-linear circuitry comes into picture.
From the above chapter it can be concluded that :-

1. The power transfer increases with the increase in number of IRS elements and vice versa.
2. The increase in number of BS antennas increases the power transfer to the UAV and decreases the outage probability.
3. The outage probability increases when the CSI(Channel state information) is unknown at the BS which decreases overall performance of the system.
4. The receive architecture should be adjusted according to the priority of the power requirement for the UAV.
5. To increase the power harvesting at the UAV maximum portion of the received power should be harvested along with the time duration for its harvesting which will decrease the outage probability for energy harvesting.

4 CONCLUSION AND FUTURE WORK

4.1 Conclusion

Hence from the above observations it is clear that energy received increases with increase in number of IRS elements for both SISO and MISO system. The received energy increases with increase in elevation angle as the probability of UAV to be in LoS increases as elevation angle increases so the energy can be more efficiently transmitted from direct path which is always the most contributing path in energy transfer. In MISO and SISO case outage probability decreases with the increase in number of IRS elements and increase in number of BS antennas. Energy transfer is always more when the CSI is known to BS as compared to energy transfer when CSI is unknown to BS. Non-linear energy harvesting always gives a clear picture about the practical power harvested as compared to linear energy harvesting.

4.2 Future Work

In the thesis work we compared results of model when CSI is known to BS antennas and when CSI is not known in MISO case. But work for MIMO is an important factor to work upon in future. Along with this here we have considered continuous phase shifts in optimization but practically discrete phase shifting circuits are only present so the work on this aspect will be useful for practical systems to build upon. Some work needs to be done on heterogeneous network where cellular network is on ground and UAV is present in the sky and study the interference of energy transfer on cellular network.

A APPENDIX

A.1 Model to calculate Distance and Elevation angle

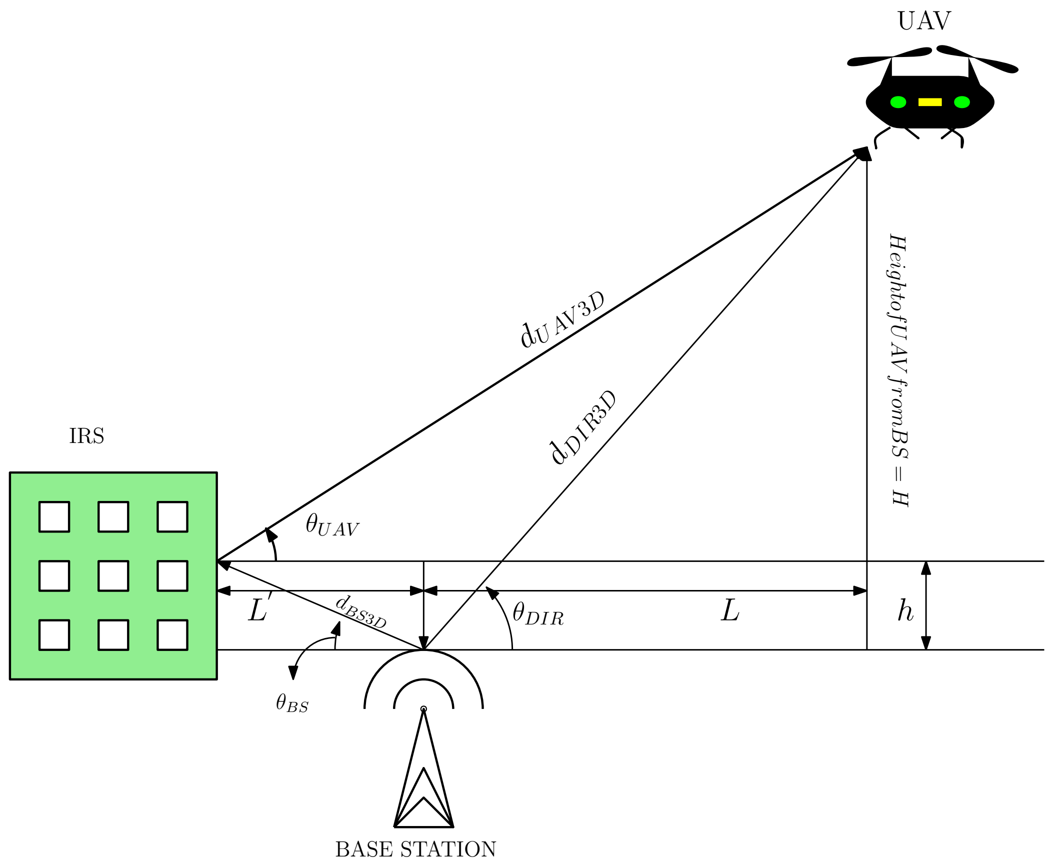

Figure 18: Model to calculate Distance and Elevation angle

The above model will find the distance and elevation angle between IRS to UAV using LoS channel (BS-UAV) parameters i.e. distance and elevation angle between BS and UAV.

The horizontal distance between BS-UAV and BS-IRS is given by:-

$$L = d_{DIR3D} \cos(\Theta_{DIR}) \tag{36}$$

$$L^{'} = d_{BS3D} \cos(\Theta_{BS}) \tag{37}$$

Vertical height of UAV from BS,

$$H = d_{DIR3D} \sin(\Theta_{DIR}) \tag{38}$$

The elevation angle of UAV w.r.t.IRS is ,

$$\Theta_{UAV} = \tan^{-1}[\frac{d_{DIR3D} \sin(\Theta_{DIR}) - d_{BS3D} \sin(\Theta_{BS})}{d_{DIR3D} \cos(\Theta_{DIR}) + d_{BS3D} \cos(\Theta_{BS})}] \tag{39}$$

The distance between IRS and UAV is given by:-

$$d_{UAV3D} = \frac{d_{DIR3D} \cos(\Theta_{DIR}) + d_{BS3D} \cos(\Theta_{BS})}{\cos(\Theta_{UAV})} \tag{40}$$

References

[1] Akram Al-Hourani, Sithamparanathan Kandeepan, and Abbas Jamalipour. Modeling air-to-ground path loss for low altitude platforms in urban environments. In *2014 IEEE Global Communications Conference*, pages 2898–2904, 2014.

[2] Akram Al-Hourani, Sithamparanathan Kandeepan, and Simon Lardner. Optimal LAP altitude for maximum coverage. *IEEE Wireless Communications Letters*, 3(6):569–572, 2014.

[3] Ertugrul Basar. Transmission through large intelligent surfaces: A new frontier in wireless communications. In *2019 European Conference on Networks and Communications (EuCNC)*, pages 112–117, 2019.

[4] Elena Boshkovska, Derrick Wing Kwan Ng, Nikola Zlatanov, and Robert Schober. Practical non-linear energy harvesting model and resource allocation for SWIPT systems. *IEEE Communications Letters*, 19(12):2082–2085, 2015.

[5] Stephen Boyd and Lieven Vandenberghe. *Convex optimization*. Cambridge university press, 2004.

[6] Nesrine Cherif, Mohamed Alzenad, Halim Yanikomeroglu, and Abbas Yongacoglu. Downlink coverage and rate analysis of an aerial user in vertical heterogeneous networks (VHetNets). *IEEE Transactions on Wireless Communications*, 20(3):1501–1516, 2021.

[7] Bruno Clerckx, Rui Zhang, Robert Schober, Derrick Wing Kwan Ng, Dong In Kim, and H. Vincent Poor. Fundamentals of wireless information and power transfer: From RF energy harvester models to signal and system designs. *IEEE Journal on Selected Areas in Communications*, 37(1):4–33, 2019.

[8] Shanshan Gao, Ke Xiong, Ruihong Jiang, Li Zhou, and Hengliang Tang. Outage performance of wireless-powered SWIPT networks with non-linear EH model in Nakagami-m fading. In *2018 14th IEEE International Conference on Signal Processing (ICSP)*, pages 668–671, 2018.

[9] Yitao Han, Shuowen Zhang, Lingjie Duan, and Rui Zhang. Cooperative double-IRS aided communication: Beamforming design and power scaling. *IEEE Wireless Communications Letters*, 9(8):1206–1210, 2020.

[10] Yuanlian Huo, Xiaopeng Xu, Jingyuan Song, and Jinling Xie. Average capacity analysis and power splitting with direct link based relaying protocol for wireless information and power transfer networks. In *2019 4th International Conference on Mechanical, Control and Computer Engineering (ICMCCE)*, pages 43–434, 2019.

[11] Salil Kashyap, Emil Björnson, and Erik G. Larsson. On the feasibility of wireless energy transfer using massive antenna arrays. *IEEE Transactions on Wireless Communications*, 15(5):3466–3480, 2016.

[12] Liang Liu, Rui Zhang, and Kee-Chaing Chua. Wireless information and power transfer: A dynamic power splitting approach. *IEEE Transactions on Communications*, 61(9):3990–4001, 2013.

[13] Abdulla Mahmoud, Sami Muhaidat, Paschalis C. Sofotasios, Ibrahim Abualhaol, Octavia A. Dobre, and Halim Yanikomeroglu. Intelligent reflecting surfaces assisted uav communications for IoT networks: Performance analysis. *IEEE Transactions on Green Communications and Networking*, 5(3):1029–1040, 2021.

[14] Zaki Masood and Yonghoon Choi. Energy-efficiency optimization for WSNs using distributed power splitting at receiver. In *2018 International Conference on Information and Communication Technology Convergence (ICTC)*, pages 1319–1323, 2018.

[15] Qingqing Wu and Rui Zhang. Intelligent reflecting surface enhanced wireless network via joint active and passive beamforming. *IEEE Transactions on Wireless Communications*, 18(11):5394–5409, 2019.

[16] Qingqing Wu and Rui Zhang. Weighted sum power maximization for intelligent reflecting surface aided SWIPT. *IEEE Wireless Communications Letters*, 9(5):586–590, 2020.

[17] Haohang Yang, Yinghui Ye, Xiaoli Chu, and Mianxiong Dong. Resource and power allocation in SWIPT-enabled device-to-device communications based on a nonlinear energy harvesting model. *IEEE Internet of Things Journal*, 7(11):10813–10825, 2020.

[18] Liang Yang, Jinxia Yang, Wenwu Xie, Mazen O. Hasna, Theodoros Tsiftsis, and Marco Di Renzo. Secrecy performance analysis of RIS-aided wireless communication systems. *IEEE Transactions on Vehicular Technology*, 69(10):12296–12300, 2020.

[19] Changsheng You and Rui Zhang. Wireless communication aided by intelligent reflecting surface: Active or passive? *IEEE Wireless Communications Letters*, pages 1–1, 2021.

[20] Yongs Zeng, Qingqing Wu, and Rui Zhang. Accessing from the sky: A tutorial on UAV communications for 5G and beyond. *Proceedings of the IEEE*, 107(12):2327–2375, 2019.

[21] Pengcheng Zhan, Kai Yu, and A. Lee Swindlehurst. Wireless relay communications using ann unmanned aerial vehicle. In *2006 IEEE 7th Workshop on Signal Processing Advances in Wireless Communications*, pages 1–5, 2006.

[22] Yafei Zhao, Qiang Li, Likun Huang, Shangjie Feng, Tao Han, and Jing Zhang. Wireless information and power transfer on cooperative multi-path relay channels. In *2016 IEEE/CIC International Conference on Communications in China (ICCC)*, pages 1–6, 2016.

[23] Özgecan Özdogan, Emil Björnson, and Erik G. Larsson. Intelligent reflecting surfaces: Physics, propagation, and pathloss modeling. *IEEE Wireless Communications Letters*, 9(5):581–585, 2020.